Ionization and high-order harmonic generation in aligned benzene by a short intense circularly polarized laser pulse

Roi Baer,[1] Daniel Neuhauser,[2] Petra R. Ždánská,[3] and Nimrod Moiseyev[3]
[1]*Institute of Chemistry and the Lise Meitner Center for Quantum Chemistry, Hebrew University of Jerusalem, Jerusalem 91904, Israel*
[2]*Department of Chemistry and Biochemistry, University of California at Los Angeles, Los Angeles, California 90025, USA*
[3]*Department of Chemistry, Technion–Israel Institute of Technology, Haifa 32000, Israel*
(Received 27 April 2003; published 20 October 2003)

We present a first-principles study of ionization and high-order harmonic generation by benzene aligned in the polarization plane of a short circularly polarized laser pulse. Time-dependent density-functional theory within the adiabatic local-density approximation is employed to describe the 30 valence-electron dynamics in three dimensions. The multielectron approach enables us to study the effect of very strong laser fields, $10^{14}-10^{15}$ W cm^{-2}, where multiple ionization and high-order harmonic generation interplay. Large ionization currents are formed, causing ionization of 1–4 electron charges, while strong high-order harmonic generation is observed. The well-known recollision mechanism of high-order harmonic generation plays a part for moderate laser intensities but is fully suppressed for strong laser fields. The harmonic generation spectra are characterized by two distinguishable plateaus, where the structure of the first plateau is dominated by the $6k \pm 1$ ($k=0,1,...$) selection rule. The number of harmonics in the second plateau is insensitive to the duration of the pulse. The peaks appear in pairs or in threesomes, depending on the pulse duration.

DOI: 10.1103/PhysRevA.68.043406 PACS number(s): 32.80.Rm, 42.65.Ky, 31.15.Ew, 31.15.Ar

I. INTRODUCTION

The interaction of matter with intense electromagnetic radiation is a long-standing field of basic scientific interest with considerable technological relevance. One important phenomenon attracting increased interest in recent years is high-order harmonic generation (HHG), which is a unique route to producing ultrafast pulses of soft x rays.

Most studies, experimental and theoretical, have focused attention on atomic HHG by a linearly polarized electromagnetic field [1]. The classical mechanism of this type of HHG was described by Corkum [2] and by Kulander *et al.* [3]. The strong electromagnetic field strips an electron out of the atom, and subsequently it pitches it back toward the nucleus for a violent recollision. Such a complex succession of events culminates in strong emission of high-order harmonics. This mechanism of HHG explains the cutoff at a value proportional to the ponderomotive energy and the drastic drop in yield upon deviation from linear polarization. The detailed understanding of this process has led to applications such as the recent production of attosecond pulses [4].

Recently, other types of HHG processes have been discovered in molecules. The planar benzene molecule aligned in the plane of a circularly polarized electromagnetic pulse is an example of a very different mechanism of HHG from the one described above. This system has been studied theoretically in a few recent papers. Selection rules for HHG by a circularly polarized infinite pulse in symmetric molecules have been derived by Alon, Averbukh, and Moiseyev [5]. High-order harmonics given by the $6k \pm 1$ ($k=0,1,...$) selection rule show up for the sixfold symmetric benzene molecule aligned perpendicular to the propagation axis of the field. The same authors showed in their subsequent study [6] that molecular HHG by a circularly polarized laser field is a result of ''bound-bound'' transitions rather than ''bound-continuum'' transitions, which dominate in the Corkum-Kulander recollision mechanism for atoms in a linearly polarized field. To date, the most comprehensive numerical studies of HHG in benzene have been done in the scope of a one-electron two-dimensional model of discrete cylindrical symmetry, introduced by Ceccherini *et al.* for a temporally finite pulse [7,8]. A rich spectral structure dominated by the aforementioned selection rule has been reported. Recently, this model has been employed to study HHG in benzene by an infinite pulse [9] by using the approach of complex-scaled coordinates to calculate the Floquet resonant states. The HHG selection rules have been confirmed numerically and their dominance has been established even when the polarization is not fully circular and/or the molecular alignment is not perfect. The HHG mechanism was confirmed as due to ''bound-bound'' transitions when the exact HHG spectrum was found to be similar to the HHG spectrum obtained from a truncated basis set including the benzene bound states only.

A directly relevant measurement of HHG in aligned benzene using a circularly polarized laser field has yet to be reported. The HHG spectra of benzene and other small organic molecules have been measured for several polarization ellipticities using 780 nm 70 and 240 fs laser pulses and strong laser intensities $10^{14}-2\times10^{15}$ W cm^{-2} by Hay *et al.* [10]. Odd high-order harmonics were detected up to the 15th order. It has been suggested that molecular fragmentation is taking part in the molecular HHG process for long pulses of 240 fs.

Since the previous theoretical studies were conceived within one-electron approaches, they were limited to moderate laser fields, up to 10^{13} W cm^{-2}, where no more than one electron is ionized. In this paper, we study the system on an *ab initio* level, constructing the time-dependent many-electron wave function. This allows us to study the molecular interaction with strong laser fields, $10^{14}-10^{15}$ W cm^{-2}, when HHG and multiple ionization interplay. Although for

very long laser pulses, more than 100 optical cycles, the effect of the finite pulse envelope at high frequencies can be studied using an adiabatic theory [11], in the present case, a realistic frequency of around 800 nm cannot be considered high and an exact time-dependent evolution must be employed.

Our study brings realistic results to light, to serve as a roadmap for experimentalists and to examine the considerations of the molecular HHG mechanism. We show that the selection rules are observable in short laser pulses and that the HHG is effective despite strong ionization. We calculate the electronic current during the pulse and show that recollisions are present for moderate laser intensity, while they diminish completely for strong laser intensity. These results partly support the previous considerations that the HHG mechanism in molecules caused by strong circularly polarized radiation is caused by ''bound-bound'' rather than ''bound-continuum'' transitions [6]. Nevertheless, for moderate laser intensity, even for a circularly polarized field, the ''bound-continuum'' transitions provide an additional channel for HHG.

Time-dependent density-functional theory (TDDFT) within the adiabatic local-density approximation is used for simulating the real-time many-electron dynamics. TDDFT is finding a growing number of applications in molecular physics and theoretical chemistry, being a fine blend of the ''doable'' and the ''accurate.'' The use of TDDFT is typically done in the frequency domain [12,13]. Using it in the real-time domain is less popular yet allows treating a wide variety of nonperturbative processes [14]. Some applications of TDDFT in real time were published by Baer [15–17]. Recently, Baer showed how it is possible to compute nonadiabatic couplings using real-time TDDFT [18], and Baer and Neuhauser calculated the ac and dc conductance of a molecular wire [17,19]. Baer and Cederbaum have recently shown the utility of real-time TDDFT for calculation of photoabsorption cross sections in molecules and clusters [20]. TDDFT in real time is rapidly gaining popularity, and already several groups have published important studies in the field of laser-molecule interactions, including ionization processes in diatomics [21] and metal clusters [22] and HHG [23,24] in diatomics.

The structure of the paper is as follows. In Sec. II we present the calculation method and relevant details concerning the application. Results concerning ionization and HHG are given in Secs. III and IV, respectively, followed by a summary in Sec. V.

II. METHOD

A. Time-dependent density-functional theory

All observables reported below are calculated within the time-dependent density-functional theory framework [25] with the adiabatic local-density approximation. The time-dependent density $n(\mathbf{r},t)$ is represented as a sum of squared orbitals:

$$n(\mathbf{r},t)=2\sum_{n=1}^{N_e/2}|\psi_n(\mathbf{r},t)|^2. \tag{1}$$

At time $t=0$ the density is the ground-state density and the orbitals $\psi_n(\mathbf{r},t=0)$ are the Kohn-Sham orbitals [26] within the local-density approximation (LDA). At later times the orbitals are determined by solving the time-dependent Kohn-Sham equations:

$$i\hbar\frac{\partial\psi_n}{\partial t}=[\hat{H}_{\mathrm{KS}}[n]-e\vec{E}(t)\cdot\vec{\mathbf{r}}]\psi_n, \tag{2}$$

where $\vec{E}(t)$ is the time-dependent electric field, e the electron charge, and $\vec{\mathbf{r}}$ the electron position. $\hat{H}_{\mathrm{KS}}[n]$ is the Kohn-Sham Hamiltonian:

$$\hat{H}_{\mathrm{KS}}[n]=-\frac{\hbar^2}{2\mu_e}\nabla^2+v_{\mathrm{nuc}}(\mathbf{r})+\int\frac{n(\mathbf{r}',t)}{|\mathbf{r}'-\mathbf{r}|}d^3r'+v_{\mathrm{xc}}[n](\mathbf{r}). \tag{3}$$

Here, μ_e is the electron mass and v_{nuc} is the electrostatic potential resulting from the attraction of electrons to the nuclei of the molecule. Equation (1) is a one-electron dynamical equation which resembles the Schrödinger equation. Yet, because the Hamiltonian is a functional of the time-dependent density $n(\mathbf{r},t)$, the electrostatic interactions, correlation effects, and exchange interactions can in principle be accurately accounted for, provided the ''exchange-correlation potential'' $v_{\mathrm{xc}}[n](\mathbf{r})$ is known. In practice, this latter quantity is approximated, for example, the adiabatic local-density approximation used in this work assumes that the potential at point $\mathbf{r}$ and time t depends only on the density at this place and time:

$$v_{\mathrm{xc}}[n](\mathbf{r})=V(n(\mathbf{r},t)). \tag{4}$$

Despite the apparent crudeness of this approximation, it is known to obey many of the sum rules obeyed by the accurate functional. The LDA is frequently found to yield reasonably accurate excitation molecular energies.

B. Application details

We place a benzene molecule containing all 30 valence electrons in a large three-dimensional (3D) rectangular cell of dimensions $L_x=L_y=L=48a_0$ and $L_z=12a_0$. Within the cell a 3D grid is used to describe all 15 Kohn-Sham orbitals. The grid spacing used is $\Delta x=\Delta y=\Delta z=0.5a_0$, corresponding to a kinetic energy cutoff value of about $20E_h$. The combination of the grid spacing with the Troullier-Martins pseudopotentials [27] produced by the PP98 program [28] is reasonable, and convergence of the calculations was checked against results with slightly larger grid spacings. The kinetic energy operator is applied using fast Fourier transform (FFT). The Coulombic integral in Eq. (3) is also efficiently performed using FFT. Ewald images are screened according to the method of Martyna and Tuckerman [29]. The exchange-correlation functional is the LDA of Perdew and Wang [30] (PW92). Although more accurate methods are available [15,17], the intensive calculations demand a reasonable compromise between accuracy and efficiency. Here, the time-dependent equations were solved using a fifth-order

adaptive Runge-Kutta time step [31]. This method is stable and affords good energy and norm conservation.

In order to remove the outgoing flux, a negative imaginary potential is placed in the *x*-*y* directions [32]. The ionization current is measured before the absorption. The form of the imaginary potential is $W(\mathbf{r})=w(x)+w(y)$ with $w(x)$ defined by [33]

$$w(x)=\begin{cases} -i\,\eta(|x|-a)^n, & a\leqslant|x|\leqslant L/2 \\ 0 \quad \text{otherwise.} \end{cases} \tag{5}$$

The parameters used were $n=3$, $a=9a_0$, and $\eta=1.5\times10^{-4}E_h a_0^{-3}$.

Within this model we optimized the geometry of the molecule, obtaining the known hexagonal benzene geometry with the following bond lengths: $R_{\mathrm{CC}}=1.4$ Å and $R_{\mathrm{CH}}=1.1$ Å. The absorption spectrum is calculated by Fourier transforming a TDDFT signal that simulates the response of the system to a weak electric signal. The main absorption line is found at 178 nm, in excellent agreement with experiment [34] and with a previously reported TDDFT calculation of Yabana and Bertsch [35].

The circularly polarized intense laser field was represented as a time-dependent potential [Eq. (2)], where

$$\vec{E}(t)=E_0\sin^2(\pi t/T)(\hat{\mathbf{x}}\sin\omega t+\hat{\mathbf{y}}\cos\omega t). \tag{6}$$

Here, E_0 is the maximal electric field, T is the pulse duration, and ω is the central frequency. In the present calculation we simulated an 800 nm laser pulse. We checked two pulse durations, one of 10 and the other of 20 cycles ($T=26.7$ and 53.4 fs).

The HHG is deduced using the following procedure. During the dynamical propagation, the time-dependent dipole $\vec{\mu}(t)=e\int n(\vec{r},t)\vec{r}\,d^3r$ is recorded at time intervals of $\Delta t=0.5$ a.u. The power spectrum of the dipole acceleration $\ddot{\mu}_x$ in a given direction yields the predicted HHG spectra:

$$s_x(\omega)\propto\omega^4\left|\int\mu_x(t)e^{i\omega t}dt\right|^2. \tag{7}$$

If high harmonics are to be resolved, the function $\vec{\mu}(t)$ must be terminated smoothly after the pulse ends. We do this by multiplying $\vec{\mu}(t)$ prior to the Fourier transform by an envelope $s(t,\tau)$, forcing it to decay to zero when the pulse terminates:

$$\tilde{\vec{\mu}}(t)=\vec{\mu}(t)s(t,\tau), \tag{8}$$

where

$$s(t,\tau)=\begin{cases} 1, & t<\tau \\ \sin^2[\pi(T-t)/2(T-\tau)], & \tau<t<T \\ 0 \quad \text{otherwise,} \end{cases} \tag{9}$$

with $\tau=3T/4$. If we do not use this function, we get spurious results for the very high harmonics which have a low intensity and are therefore especially sensitive to any abrupt discontinuity of the signal. The exact form of smoothly cutting the signal is immaterial, and in fact we have assured that the results are insensitive to the exact value of τ used.

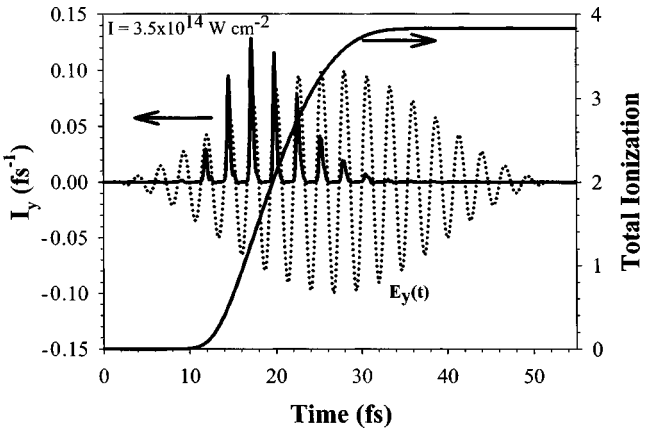

FIG. 1. The total ionization N and the ionization current I_y at $y=7a_0$ as functions of time for a strong circularly polarized laser pulse (3.5×10^{14} W cm^{-2}). Superimposed (dotted): the y component of the electric field E_y (in arbitrary units). Pulse duration is 20 cycles. The recollision event is not observed. Ionization almost ceases by the time the pulse reaches maximal intensity.

III. TIME-DEPENDENT IONIZATION

The time-dependent calculation allows a detailed analysis of the ionization process as it evolves with time. The study of the ionization process allows an indirect study of the HHG mechanism by examining the recollision process. Thus we calculate the ionization current I_y in the y direction near the hydrogen atoms, at $y_0=7a_0$. This current changes with time, and is defined as $I_y(y_0)=\int J_y(x,y_0,z,t)dx\,dz$, where $\mathbf{J}$ is the one-electron current density:

$$\mathbf{J}(\mathbf{r},t)=\frac{1}{2\mu_e}\sum_{n=1}^{N_e}\langle\psi(t)|\,\delta(\mathbf{r}-\hat{\mathbf{r}}_n)\hat{\mathbf{p}}_n+\hat{\mathbf{p}}_n\delta(\mathbf{r}-\hat{\mathbf{r}}_n)\,|\psi(t)\rangle. \tag{10}$$

Here $\psi(t)$ is the many-body wave function. The current density in DFT is given by the corresponding sum over the Kohn-Sham orbitals. Another quantity used to study the ionization process is the ''total ionization'' given by

$$N(t)=\int n(\mathbf{r},t=0)d^3r-\int n(\mathbf{r},t)d^3r. \tag{11}$$

Two different cases are studied, ionization by a strong laser pulse (3.5×10^{14} W cm^{-2}), demonstrated in Fig. 1, and ionization by a moderate laser pulse (3.2×10^{13} W cm^{-2}), Fig. 2.

For a strong laser field, every time the electric field points out of the molecular core [$E_y(t)>0$, dotted curve in Fig. 1], the ionization current peaks [$I_y(t)=$max, dotted curve in that figure]. The ionization current acquires only positive values because that part of the molecular electronic charge that is torn away from the molecule and thrown out in the positive y direction never returns. The recollision events, which are the key point in the well-known HHG mechanism

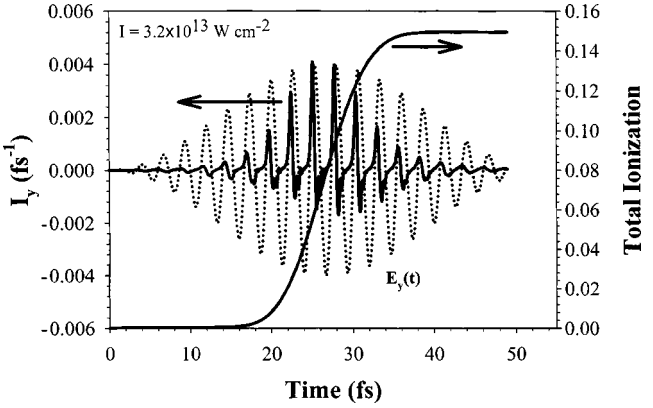

FIG. 2. Same as Fig. 1 for a moderate circularly polarized laser pulse (3.2×10^{13} W cm^{-2}). Some of the flux thrown past the point at $y=7a_0$ recollides with the molecular core. The ionization rate follows the pulse strength.

in atoms, are entirely missing for HHG in a strong circularly polarized laser field. The global maximum of ionization current shows that the ionization rate reaches a maximum well before the pulse reaches maximum intensity. This is a direct result of the high efficiency of the ionization process in this regime: the charge that can be ionized is ionized quickly—before the field reaches maximal strength.

For moderate laser fields, the behavior is radically different, as seen in Fig. 2: the ionization current acquires negative values also, when the electric field does not point directly out of the benzene molecule, $E_y\neq\max$. An appreciable amount of the current flowing outward when the field is in the y direction is pulled back into the molecule. Note that the driving field is still positive, $E_y>0$, when the ionic current changes its sign. Therefore, it is rather the attractive pull of the electrons to the ion that causes the recollision and prevents immediate ionization. We conclude that in moderate circularly polarized laser fields the HHG spectrum has non-negligible contributions from the bound-continuum transitions. Figure 2 also shows that the maximal ionization rate is obtained at maximal field strength in moderate laser fields, which differs from the case of a strong laser pulse.

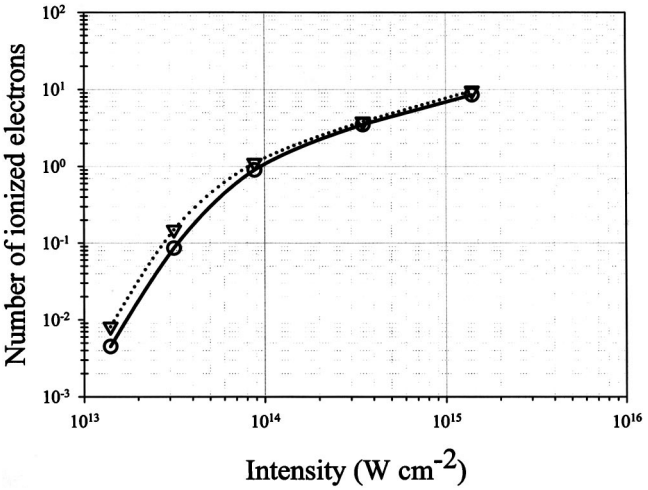

FIG. 3. The total ionization as a function of intensity for 10- (circles) and 20- (triangles) cycle pulses. For convenience a spline is drawn between the points.

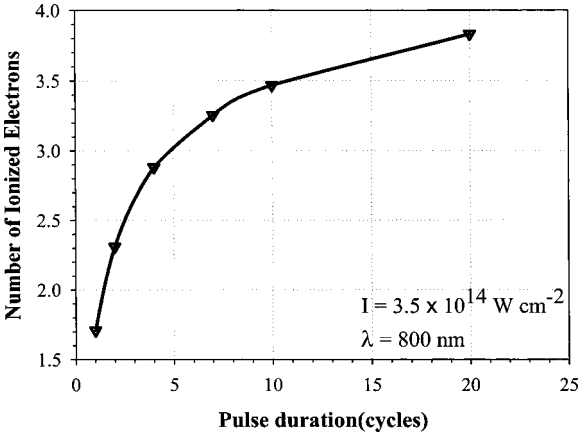

FIG. 4. The ionization as a function of pulse duration for a given intensity and wavelength.

The dependence of the total ionization on the intensity and pulse duration is shown in Fig. 3 for pulse durations of 10 and 20 optical cycles ($T=26.7$ and 53.4 fs). A strong dependence of the number of ionized electrons on intensity is observed. The pulse duration makes a difference for low intensities but not for high ones. This is explained by the previous observation that, at high intensities the ionization ceases well before the pulse is over, but for low intensities, where ionization continues throughout, we would expect a linear dependence on the pulse duration.

The total ionization as a function of pulse duration is shown in detail in Fig. 4 for strong laser fields, where a substantial nonlinear behavior is observed.

IV. HARMONIC GENERATION

The HHG spectra in aligned benzene caused by a circularly polarized ten-cycle pulse are shown in Fig. 5 for several pulse intensities, ranging from moderate, 1.4×10^{13}, to

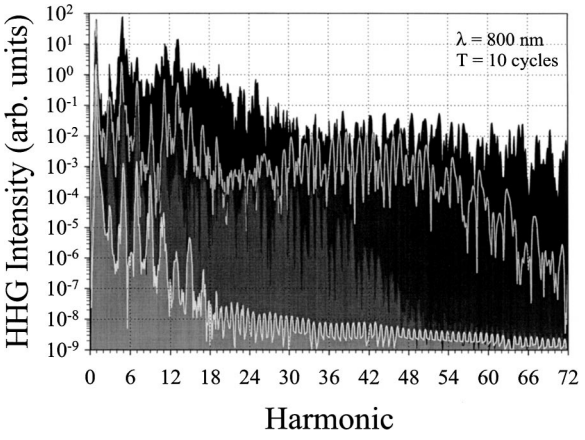

FIG. 5. The HHG spectrum of oriented benzene exposed to circularly polarized light. Results of a ten-cycle pulse. The pulse strengths are 140, 35.1, 8.77, and 1.40×10^{13} W cm^{-2}. Note that numerical noise is significant at intensities below 10^{-7}.

TABLE I. Laser intensities where 9th, 11th, and 13th high-order harmonics join the first plateau: HHG in aligned benzene by ten-cycle circularly polarized laser pulse by present TDDFT study (column 2); HHG in aligned benzene by infinite laser pulse by two-dimensional one-electron model, Ref. [9] (column 3); HHG in nonaligned benzene by 26-cycle linearly polarized laser pulse by experiment, Ref. [10] (column 4).

Harmonic	TDDFT	Ref. [9], Fig. 4	Ref. [10] Fig. 3(d)
9	1.40×10^{13}	2.37×10^{13}[a]	7×10^{14}
11	8.77×10^{13}	3.00×10^{13}	1×10^{15}
13	3.51×10^{14}	5.50×10^{13}	1×10^{15}

[a]The ninth high-order harmonic is obtained by linear interpolation as it is forbidden by selection rules.

strong laser intensity, 1.4×10^{15} W cm^{-2}. Despite the high efficiency of the ionization process, which is discussed in the previous section, the yield of HHG increases as the laser intensity grows. The HHG spectra obtained using high-intensity short laser pulses ($E_0 \geqslant 8.77\times10^{13}$ W cm^{-2}) acquire a double-plateau structure, where the first plateau ends in a gap of HHG and after this gap a long succession of intense lines rises to the second plateau (note: the gap between the plateaus is more clearly observed in Figs. 7–9 below).

The increasing length of the first plateau with the laser intensity is apparent from the critical laser intensities where the 9th, 11th, and 13th high-order harmonics join the first plateau, Table I. The TDDFT results for the ten-cycle circularly polarized pulse (column 2) are compared with the previous one-electron two-dimensional model for an infinite pulse (column 3) [9], and with the experimental data for a 26-cycle linearly polarized pulse (column 4) [10]. Based on Table I, we predict that the HHG by a circularly polarized field in aligned benzene will provide a comparable or longer first plateau than HHG in nonaligned molecules caused by a linearly polarized pulse. It is also shown in Table I that the previous results using the one-electron approximation provided relatively good estimates of the plateau length; however, they overestimated the plateau increase with intensity.

For the first plateau, the symmetry selection rule ($6k \pm 1$), $k=1$, 2, 3, dominates the spectral structure, even for short laser pulses. The symmetry selection rule gets more pronounced with the increasing duration of the laser pulse, as shown in Table II, where the ratios of intensities between low harmonic peaks are presented. The intensities of the

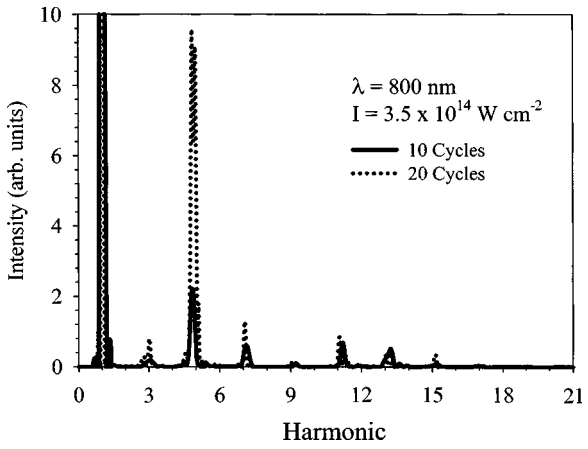

FIG. 6. The HHG spectra for 10- and 20-cycle pulses. Peaks are seen at odd harmonics, yet the $6k\pm1$ harmonics are considerably stronger.

''symmetry-forbidden'' peaks (3, 9, and 15) vs ''symmetry-allowed'' peaks are shown in the three last columns of Table II. The ratios, which are significantly higher than unity, evidence the aforementioned selection rule. On the other hand, the measurement due to Hay *et al.* [10] shows clearly that linearly polarized HHG does not obey these selection rules, as expected (Table II).

The effect of pulse duration on the first-plateau harmonics is further studied in Fig. 6, where the HHG spectra for a laser intensity of 3.5×10^{14} W cm^{-2} are shown for 10- and 20-cycle pulses. The dominance of the symmetry-allowed peaks is clearly shown; and the full width at half maximum of the HHG peaks gets narrower for the longer laser pulse. The striking difference is the yield of HHG spectra, which is very sensitive to the duration.

The short-pulse HHG is characteristized by small shifts of peaks from integer harmonics in the first plateau. The effect is studied in Table III, showing that the fifth harmonic is detuned to the red while other peaks are detuned to the blue. In general, the phenomena get weaker when the pulse is longer (except for the fifth harmonic).

This shift phenomenon can be explained within the non-Hermitian quantum mechanical theory for HG spectra recently derived by Moiseyev and Lein [36]. The shifted odd harmonics result from interference between two nondegenerate quasienergy (QE) Floquet states. These states must also be eigenstates of the dynamical symmetry operator and they are degenerate with respect to it. There is no reason for the two QE states to have the same lifetime, so when the dura-

TABLE II. The ratio between intensities of peaks at 3, 5, 7, and 9 harmonics. First three lines, circularly polarized laser pulse, the intensity is 3.5×10^{14} W cm^{-2}. Fourth line, experimental results for a linearly polarized pulse, ratios taken from Fig. 2 of Ref. [10].

Cycles	Polarization	(5/7)	(7/11)	(5/3)	(11/9)	(7/9)
4	Circular	3.4	1.1	5.4	2.9	3.2
10	Circular	3.2	0.9	11.0	6.8	6.1
20	Circular	7.0	1.5	12.4	5.0	7.5
Ref. [10]	Linear		1.25		0.5	0.5

TABLE III. The location of the harmonic peak for different pulse lengths. Note that the low-intensity peaks in the harmonic generation spectra are obtained due to the finite duration of the laser pulse. In the cw case they are symmetry-forbidden harmonics

Harmonic	4 cycle	10 cycle	20 cycle
3	3.01	3.01	3.01
5	4.76	4.91	4.86
7	7.26	7.11	7.06
9	8.77	9.22	9.06
11	11.52	11.22	11.07
13	13.53	13.23	13.03

tion of the laser pulse is sufficiently long only one QE state controls the photoinduced dynamics (the longest-lived QE resonance state), and the ''line-shift'' effect is suppressed. However, for sufficiently short pulses both these states affect the HG spectrum and this results in a shift from integer harmonics.

A second plateau of harmonics is observed for very strong laser fields for short laser pulses. Note that for moderate laser intensity the second plateau is missing in the HHG spectrum (Fig. 5). The lengths of the second plateau for the ten-cycle laser pulse are up to the 35th, 51st, and 72nd high-order harmonics for laser intensities 8.77×10^{13}, 3.51×10^{14}, and 1.4×10^{15} W cm^{-2}, respectively. The second plateau is not subordinate to the symmetry selection rule for a continuous wave laser, but it shows rather a peculiar structure pattern. The displacement of HHG lines from integer values is stronger than in the first plateau. Both of these features suggest that the second plateau is created due to the finite-width laser frequency.

The appearance of a second plateau can also be explained by Floquet theory [36]. It results from the interference between two QE Floquet states which are nondegenerate eigenstates of the dynamical symmetry operator. In such a case, shifted even and odd harmonics are obtained. The results presented here show that the second plateau is less pronounced than the first where the HG spectrum conforms to the dynamical symmetry rules derived for cw lasers.

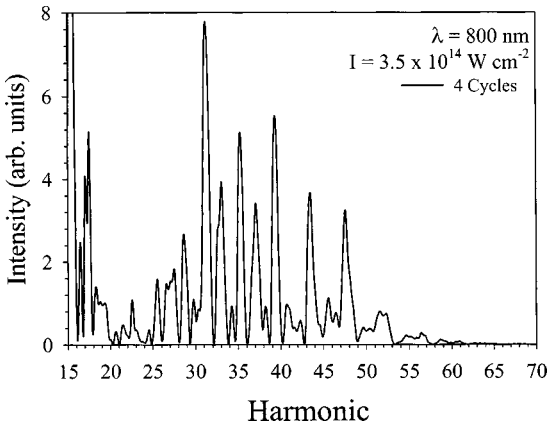

FIG. 7. Details of the HHG spectrum in the 20–70 harmonic range for a four-cycle pulse.

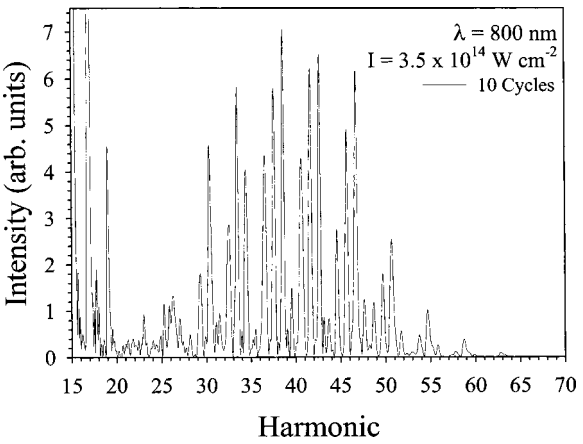

FIG. 8. Detail of the HHG spectrum at the 20–70 harmonic range for a short intense pulse of ten cycles.

The second plateau for three different pulse durations (4, 10, and 20 cycles) for laser intensity 3.5×10^{14} W cm^{-2}, is plotted in linear scale graphs in Figs. 7–9. The position of the second plateau is independent of the pulse duration, starting from the 25th and ending by the 55th high-order harmonics.

For the four-cycle laser pulse, Fig. 7, the peaks come in threesomes, a strong, a medium, and a weak peak. For example, the medium peak at 28.7, weak at 29.8, and strong at 31.2; medium at 33, weak at 34.3, and strong at 35.3; medium at 37.2, weak at 38.3, and strong at 39.3; etc. After the 40th high-order harmonic, the ''medium'' pulses are considerably degraded and one is left with only the strong pulses at 43.5, 47.5, and 51.5.

On the whole, the same structure appears also for the ten-cycle pulse, Fig. 8. The threesome character of the peaks is very striking, degrading after the 45th harmonic. It is interesting to note that most peaks appear not at integer harmonics but at half odd integer harmonics.

When the pulse is longer, e.g., 20 cycles (Fig. 9), the threesome phenomenon is degraded, and a pair pattern appears. Two intense peaks are followed by two weak ones. The peaks are now only slightly displaced from integer harmonics.

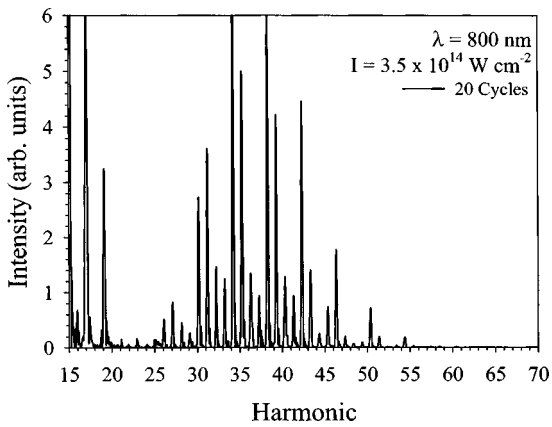

FIG. 9. Detail of the HHG spectrum at the 20–70 harmonic range for a short intense pulse of 20 cycles.

V. SUMMARY

We have presented an *ab initio* simulation of the interaction of a temporally short and intense circularly polarized laser pulse with an aligned benzene molecule. We have studied two processes in this system, ionization and HHG yields.

As for ionization, we found that for field strengths larger than 1×10^{14} W cm^{-1} the intensity is sufficiently strong so that the electrons pulled out of the molecule do not return to it. For fields weaker than this limit a different behavior is observed: some of the electrons pulled out of the molecule recollide with it because of the strong attraction to the ion. For strong fields, ionization ceases well before the pulse reaches maximum, while for pulses of maximal strength smaller than 1×10^{14} W cm^{-2} the ionization continues throughout. The immediate conclusion is support for the conjecture of Averbukh, Alon, and Moiseyev [6]: for strong laser intensity, molecular HHG by a circularly polarized field is not associated with the ionized electrons, but with the bound electrons that do not ionize. For moderate laser intensities, however, the recollision mechanism creates an additional channel even for molecular HHG by circularly polarized fields.

The HHG yield has been studied for several laser intensities of short laser pulses, of durations 4, 10, and 20 cycles. The HHG spectra show a single plateau for moderate laser intensity and a double-plateau structure for very strong laser intensities. The length of the first plateau is comparable both with the experimental result of Hay *et al.* [10], using 70 fs linearly polarized laser pulses, and with the previous one-electron model study [9]. Based on our study we predict that the HHG in aligned benzene by a circularly polarized field will yield a similar or longer plateau than the HHG in nonaligned benzene by a linearly polarized field. The first plateau is clearly dominated by the $(6k\pm1)$ selection rule, holding exactly for infinite circular pulses [5]. The $(6k\pm1)$ selection rule is uniquely specific for the circularly polarized field, being absent in previous experiments with nonaligned benzene in a linearly polarized field [10]. The presence of the second plateau is attributed to the nonzero frequency width of the finite laser pulses, since unusual structure and noninteger harmonics are observed in the second plateau. The second plateau allows generation of very high-order harmonics up to the 72nd order using the laser intensity 1.4×10^{15} W cm^{-2}.

An important question is the role of multielectron effects. In relatively weak pulses we expect weak multielectron effects. In medium fields, there is interplay between HHG formed from bound-bound and that formed from bound-continuous transitions. It is possible that the bound-bound transitions are made by ''different'' electrons than those made by the bound-continuous transitions. This leads to an interesting multielectron mechanism. In yet stronger fields, several electrons are ionized during the pulse. This leads to significant time-dependent unscreening of the ionic cores, which has strong effects on the HHG. In connection with the issue of multielectron effects, an interesting question is the origin of the second plateau, appearing after the gap. This probably cannot be attributed to multielectron effects, since a similar double-plateau structure was observed in a single-active-electron calculation [Fig. 4(b) of [8]].

The intricate process of harmonic generation by circularly polarized radiation shining on aligned ring molecules still awaits experimental measurements. The results of the present article can serve as a ''road map'' for such an experiment. The experimental results, on the other hand, can be used to assess the adequacy of TDDFT for understanding and simulating HHG processes.

ACKNOWLEDGMENTS

This work was supported by the German Israel Foundation (GIF) and the Basic Research Foundation administered by the Israeli Academy of Sciences and Humanities.

[1] J. A. Armstron, N. Bloembergen, J. Ducuing, and P. S. Persham, Phys. Rev. **127**, 1918 (1962).
[2] P. B. Corkum, Phys. Rev. Lett. **71**, 1994 (1993).
[3] K. C. Kulander, K. J. Schafer, and J. L. Krause, in *Super-Intense Laser-Atom Physics*, Vol. 316 of *NATO Advanced Study Institutes, Series B: Physics*, edited by B. Piraux, A. L'Huillier, and K. Rzazewski (Plenum, New York, 1993).
[4] M. Drescher, M. Hentschel, R. Kienberger, G. Tempea, C. Spielmann, G. A. Reider, P. B. Corkum, and F. Krausz, Science **291**, 1923 (2001).
[5] O. E. Alon, V. Averbukh, and N. Moiseyev, Phys. Rev. Lett. **80**, 3743 (1998).
[6] V. Averbukh, O. E. Alon, and N. Moiseyev, Phys. Rev. A **64**, 033411 (2001).
[7] F. Ceccherini, D. Bauer, and F. Cornolit, J. Phys. B **34**, 5017 (2001).
[8] F. Ceccherini and D. Bauer, Phys. Rev. A **64**, 033423 (2001).
[9] P. Zdanska, V. Averbukh, and N. Moiseyev, J. Chem. Phys. **118**, 8726 (2003).
[10] N. Hay, R. de Nalda, T. Halfmann, K. J. Mendham, M. B. Mason, M. Castillejo, and J. P. Marangos, Phys. Rev. A **62**, 041803 (2000).
[11] D. Barash, A. E. Orel, and R. Baer, Phys. Rev. A **61**, 013402 (2000).
[12] E. K. U. Gross and W. Kohn, Phys. Rev. Lett. **55**, 2850 (1985).
[13] M. Stener, G. Fronzoni, D. Toffoli, and P. Decleva, Chem. Phys. **282**, 337 (2002).
[14] K. Yabana and G. F. Bertsch, Phys. Rev. B **54**, 4484 (1996).
[15] R. Baer, Phys. Rev. A **62**, 063810 (2000).
[16] R. Baer, in *Multiscale Computational Methods in Chemistry and Physics*, edited by A. Brandt, J. Bernholc, and K. Binder (IOS, Amsterdam, 2001), Vol. 177.
[17] R. Baer and R. Gould, J. Chem. Phys. **114**, 3385 (2001).
[18] R. Baer, Chem. Phys. Lett. **264**, 75 (2002).
[19] R. Baer and D. Neuhauser, Int. J. Quantum Chem. **91**, 524 (2003).
[20] R. Baer and L. S. Cederbaum (unpublished).
[21] M. Petersilka and E. K. U. Gross, Laser Phys. **9**, 105 (1999).

[22] F. Calvayrac, A. Domps, P. G. Reinhard, E. Suraud, and C. A. Ullrich, Eur. Phys. J. D **4**, 207 (1998).
[23] X. Chu and S. I. Chu, Phys. Rev. A **63**, 023411 (2001).
[24] X. Chu and S. I. Chu, Phys. Rev. A **64**, 063404 (2001).
[25] E. Runge and E. K. U. Gross, Phys. Rev. Lett. **52**, 997 (1984).
[26] W. Kohn and L. J. Sham, Phys. Rev. **140**, A1133 (1965).
[27] N. Troullier and J. L. Martins, Phys. Rev. B **43**, 1993 (1991).
[28] M. Fuchs and M. Scheffler, Comput. Phys. Commun. **119**, 67 (1999).
[29] G. J. Martyna and M. E. Tuckerman, J. Chem. Phys. **110**, 2810 (1999).
[30] J. P. Perdew and Y. Wang, Phys. Rev. B **45**, 13 244 (1992).
[31] W. H. Press, S. A. Teukolsky, W. T. Vetterling, and B. P. Flannery, *Numerical Recipes in C* (Cambridge University Press, Cambridge, England, 1992).
[32] D. Neuhasuer and M. Baer, J. Chem. Phys. **90**, 4351 (1989).
[33] U. V. Riss and H. D. Meyer, J. Chem. Phys. **105**, 1409 (1996).
[34] A. Hiraya and K. Shobatake, J. Chem. Phys. **94**, 7700 (1991).
[35] K. Yabana and G. F. Bertsch, Int. J. Quantum Chem. **75**, 55 (1999).
[36] N. Moiseyev and M. Lein, J. Phys. Chem. (to be published).